Cell Reports

Report

Actinomycin D Specifically Reduces Expanded CUG Repeat RNA in Myotonic Dystrophy Models

Graphical Abstract

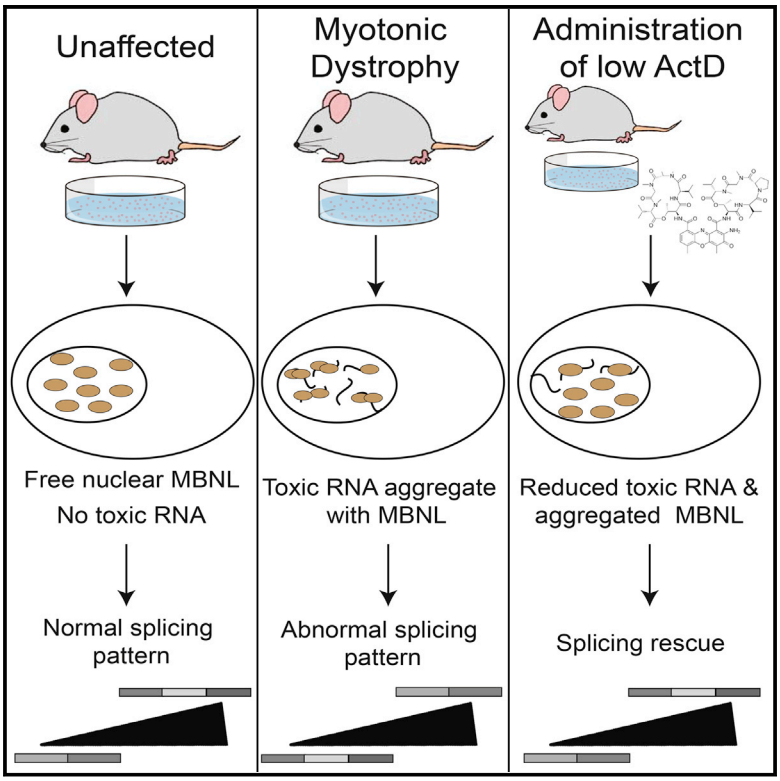

Highlights

- Actinomycin D (ActD) reduced toxic CUG RNA levels in DM1 cell and mouse models
- ActD rescued DM1-associated mis-splicing events in mice
- RNA sequencing revealed that low doses of ActD did not globally inhibit transcription
- CUG reduction and splicing rescue occurred within approved ActD therapeutic ranges

Authors

Ruth B. Siboni, Masayuki Nakamori, Stacey D. Wagner, ..., Daniel M. Cass, Matthew K. Tanner, J. Andrew Berglund

Correspondence

aberglund@ufl.edu

In Brief

Myotonic dystrophy type 1 (DM1) is caused by expression of toxic CUG RNA. Siboni and colleagues identified a low, non-toxic range over which Actinomycin D, a general transcription inhibitor, reduced CUG RNA in cell and mouse DM1 models, and rescued mis-splicing in DM1 mice. These findings validate transcription inhibition of CTG expansions as a promising therapeutic approach.

Siboni et al., 2015, Cell Reports *13*, 2386–2394
December 22, 2015
http://dx.doi.org/10.1016/j.celrep.2015.11.028

CellPress

OPEN ACCESS
CellPress

Cell Reports
Report

Actinomycin D Specifically Reduces Expanded CUG Repeat RNA in Myotonic Dystrophy Models

Ruth B. Siboni,[1,5] Masayuki Nakamori,[2,5] Stacey D. Wagner,[1] Adam J. Struck,[1] Leslie A. Coonrod,[1] Shanee A. Harriott,[3] Daniel M. Cass,[3] Matthew K. Tanner,[1] and J. Andrew Berglund[1,4,*]

[1]Institute of Molecular Biology and Department of Chemistry and Biochemistry, University of Oregon, Eugene, OR 97403, USA
[2]Department of Neurology, Osaka University Graduate School of Medicine, Osaka 565-0871, Japan
[3]Department of Chemistry, Reed College, Portland, OR 97202, USA
[4]Department of Biochemistry & Molecular Biology, Center for NeuroGenetics, College of Medicine, University of Florida, Gainesville, FL 32610, USA
[5]Co-first author
*Correspondence: aberglund@ufl.edu
http://dx.doi.org/10.1016/j.celrep.2015.11.028

SUMMARY

Myotonic dystrophy type 1 (DM1) is an inherited disease characterized by the inability to relax contracted muscles. Affected individuals carry large CTG expansions that are toxic when transcribed. One possible treatment approach is to reduce or eliminate transcription of CTG repeats. Actinomycin D (ActD) is a potent transcription inhibitor and FDA-approved chemotherapeutic that binds GC-rich DNA with high affinity. Here, we report that ActD decreased CUG transcript levels in a dose-dependent manner in DM1 cell and mouse models at significantly lower concentrations (nanomolar) compared to its use as a general transcription inhibitor or chemotherapeutic. ActD also significantly reversed DM1-associated splicing defects in a DM1 mouse model, and did so within the currently approved human treatment range. RNA-seq analyses showed that low concentrations of ActD did not globally inhibit transcription in a DM1 mouse model. These results indicate that transcription inhibition of CTG expansions is a promising treatment approach for DM1.

INTRODUCTION

Myotonic dystrophy (DM), the most common form of adult onset muscular dystrophy, is a disease characterized by (but not limited to) myotonia, muscle wasting, insulin resistance, cardiomyopathy, and cognitive dysfunctions (Ranum and Cooper, 2006; Cho and Tapscott, 2007). DM has two clinical manifestations: type 1 and type 2 (DM1 and DM2). DM1 is caused by an inherited expansion of CTG repeats in the 3′ UTR of the *DMPK* gene (Harley et al., 1992; Mahadevan et al., 1992). Unaffected individuals have between 5 and 35 CTG repeats, while those afflicted with DM1 have more than 50 and can have up to thousands of repeats (reviewed in O'Rourke and Swanson, 2009). When transcribed into RNA, the CUG repeats serve as binding sites for RNA-binding proteins, including the MBNL family of splicing factors (Miller et al., 2000). By binding to and aggregating with the CUG repeats, MBNL proteins are effectively "sequestered" away from performing their canonical functions (Ho et al., 2004; reviewed in Osborne and Thornton, 2006). Consistent with this model, in vivo fluorescent probing experiments of expanded CUG repeats demonstrated that they form nuclear aggregates, or foci, containing MBNL proteins (Fardaei et al., 2002; Ho et al., 2005).

Members of the MBNL family regulate the alternative splicing of more than 100 different transcripts, and are also involved in RNA localization and processing events (reviewed in Konieczny et al., 2014; Echeverria and Cooper, 2012). Some mRNAs that are mis-spliced in DM1, including insulin receptor (INSR), cardiac troponin T (TNNT2), and muscle-specific chloride channel (CLCN1), correspond directly or are linked to symptoms experienced by DM1 patients—insulin insensitivity, cardiac defects, and myotonia, respectively (Savkur et al., 2001; Philips et al., 1998; Mankodi et al., 2002). Although there is currently no treatment, approaches are under development that reduce or eliminate CUG:MBNL aggregates using small molecules, antisense oligonucleotides, and peptides (Warf et al., 2009; Arambula et al., 2009; Nakamori et al., 2011; Lee et al., 2012; Wheeler et al., 2012). More recently, studies have indicated that small molecules that interact with CTG-rich DNA reduce CUG RNA levels, likely through transcription inhibition (Coonrod et al., 2013). The latter finding prompted us to identify transcription inhibitors that possess high affinity and specificity for CTG-rich DNA.

Actinomycin D (ActD) is a small molecule known to bind GC-rich DNA and is naturally produced by *Streptomyces* bacteria (Waksman and Woodruff, 1940). ActD is commonly used in mRNA stability studies as a general transcription inhibitor, with common protocols using final concentrations of 1–3 μM to achieve global transcription inhibition (Bensaude, 2011; Perry and Kelley, 1970). Importantly, it is also a potent anticancer drug that has been approved by the US Food and Drug Administration since 1964 for multiple tumor types under the brand name Cosmogen. From a structural standpoint, ActD is a neutral molecule comprised of a planar phenoxazone ring with two cyclic pentapeptides (Figure 1A), and binds double and single-stranded

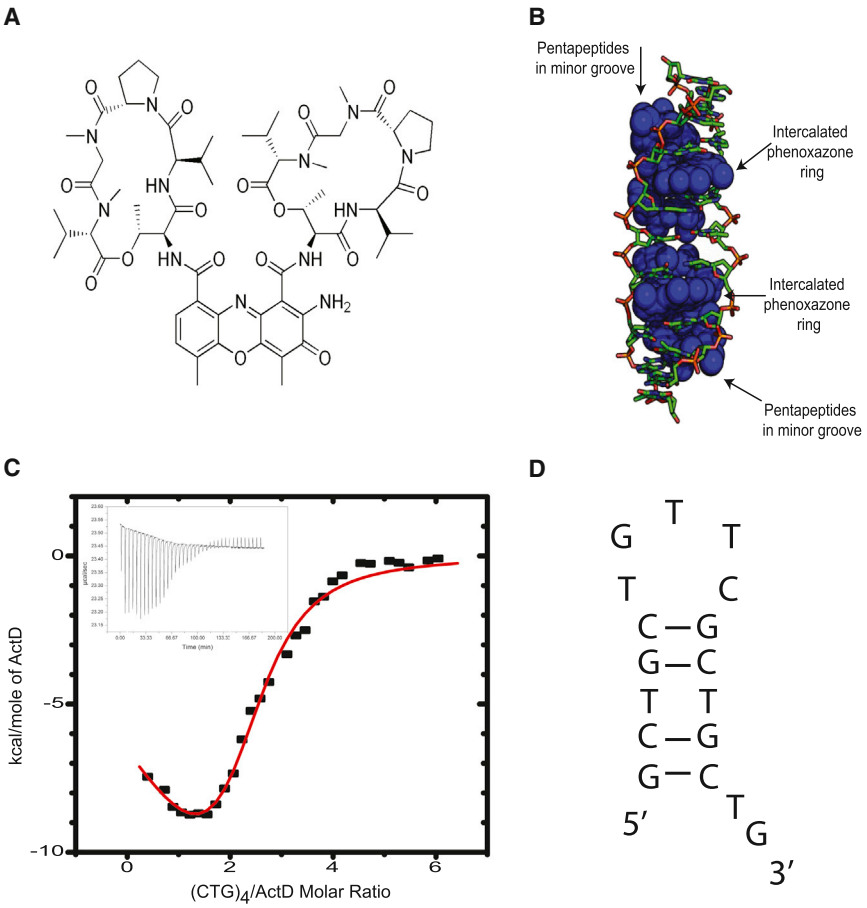

Figure 1. Biochemical Analysis of Actinomycin D Molecules Bound to CTG:CTG DNA

(A) Chemical structure of actinomycin D.

(B) Crystal structure of the 2:1 ActD-(ATGCTGCAT)2 complex (re-imaged from Hou et al., 2002). ActD molecules are in blue van der Waals representations, whereas DNA is shown in skeletal form. Intercalation of the phenoxazone ring is observed at both GpC steps, whereas pentapeptides remain within the minor groove.

(C) Representative ITC isotherm for the interaction between ActD and $(CTG)_4$. Raw heats of reaction versus time are embedded in the upper left of the graph. The average thermodynamic binding parameters when fit with the sequential binding model are $K_1 = (9 \pm 6)*10^4$, $\Delta H_1 = (7 \pm 6)*10^3$ kcal/mol, $K_2 = (2 \pm 1)*10^6$, $\Delta H_2 = (-3 \pm 1)*10^4$ kcal/mol.

(D) The lowest free energy structure of the $(CTG)_4$ sequence (Reuter and Mathews, 2010).

DNA (but not RNA) by intercalating with GpC sequences with high specificity (Müller and Crothers, 1968; Kamitori and Takusagawa, 1992). A crystal structure by Hou and colleagues demonstrated that ActD binds CTG:CTG DNA with high affinity, implicating the importance of the destabilized T:T mismatch for binding (Hou et al., 2002; Liu and Chen, 1996). Close inspection of this crystal structure reveals that the hydrophobic cyclic pentapeptides of ActD molecules are in proximity to each other when bound to CTG DNA, possibly stabilizing the ActD:DNA complex (Figure 1B). CTG:CTG DNA duplexes are a structural feature of CTG triplet repeat expansions, often the result of DNA slippage during replication (Chi and Lam, 2005; Petruska et al., 1996). Collectively, these studies suggest that ActD may possess a higher affinity for CTG repeat expansions compared to other GC-containing targets in vivo.

In this study, we determined if ActD could reduce or even completely reverse the toxic effects of transcribed CTG expansions in DM1. Using both cellular and mouse models, we demonstrated that ActD reduces CTG transcript levels and ameliorates DM1-associated mis-splicing at low concentrations. RNA sequencing (RNA-seq) analyses of a DM1 mouse model further confirmed that the concentrations of ActD necessary for significant CTG transcript reduction did not result in global transcription inhibition and rescue mis-spliced events in DM1.

RESULTS

Actinomycin D Interacts with CTG DNA Repeats, but Not CUG RNA Repeats

To ascertain whether ActD interacts with CUG RNA in a similar capacity as with CTG DNA, thermodynamic and stoichiometric properties associated with the formation of ActD complexes with $(CTG)_4$ and $(CUG)_4$ sequences were determined by isothermal titration calorimetry (ITC). At least two different types of enthalpic changes occur between $(CTG)_4$ and ActD (Figure 1C). Increasing ActD concentrations within the system resulted in an initial endothermic reaction followed by an exothermic reaction. The data were best fit with a sequential binding model, indicating cooperativity between the two binding events. The initial CTG-ActD interaction demonstrated a K_D of 10 ± 7 μM, a considerably weaker affinity than the second interaction, which produced a K_D value of 0.5 ± 0.3 μM, consistent with the lowest free-energy structure of $(CTG)_4$ containing two ActD GpC sites (Figure 1D). Taken together with previous studies that have indicated the need for a structural rearrangement of the DNA for tight binding by ActD (Hou et al., 2002; Paramanathan et al., 2012), these ITC data support an allosteric model of ActD: DNA binding. Furthermore, as ActD did not produce an enthalpic change when titrated into the $(CUG)_4$ RNA (data not shown), it is clear that ActD is unable to bind CUG RNA in vitro and thus unlikely that ActD preferentially binds CUG RNA in vivo.

Reduction of Transcripts Containing Expanded CUG Repeats with Actinomycin D

Two DM1 cell models were tested to determine the ability of ActD to reduce CUG repeat RNA levels. Previous studies demonstrated that overexpression of 960 interrupted CUG repeats by transfection into HeLa cells recapitulates DM1 mis-splicing (Ho et al., 2004; Warf et al., 2009). Northern blot analysis revealed that CUG

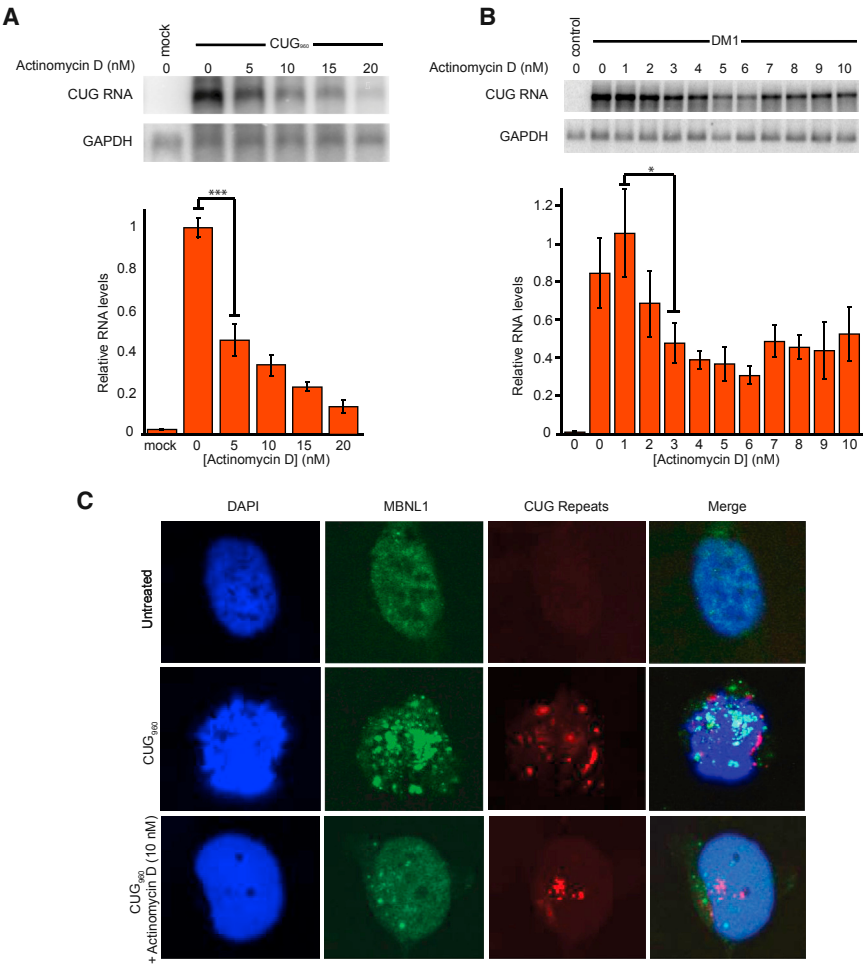

Figure 2. Actinomycin D Reduces CUG Repeat Levels in DM1 Cell Models

(A and B) CUG repeat RNA levels after ActD treatment in a DM1 HeLa cell system. Northern blot analysis and quantification demonstrate a significant decrease in CUG repeats at 5 nM within the HeLa cells and a dose-dependent decrease follows thereafter. GAPDH, a housekeeping gene, is used as a control. In DM1 patient cells, a modest increase in CUG repeats is observed after 6 nM, and CUG levels persist at that amount from 7 nM to 100 nM ActD (only data points up to 10 nM ActD are shown). Asterisks indicate level of significance ($^*p \leq 0.05$, $^{***}p \leq 0.001$). Error bars represent SD. (C) CUG ribonuclear foci formation in response to ActD treatment in HeLa cells. Top row: nuclei of untreated HeLa cells. DAPI staining of nucleus is on far left and nuclear MBNL1 staining is in the second column. These untreated cells were not transfected with CUG repeats. Middle row: transfection with CUG_{960} gives rise to ribonuclear foci in HeLa cells. Aggregation of MBNL1 and CUG repeats observed in the second and third columns, respectively. Bottom row: treatment with 10 nM ActD in HeLa cells results in decreased number and size of MBNL1 and CUG aggregates (second and third columns), and reduction of MBNL sequestration as evidence by reversion to more diffuse staining (second column).

RNA levels decreased by more than 50% ($p = 0.002$) with 5 nM ActD treatment over 18 hr, decreased by ~70% with 10 nM ActD, and a dose-dependent decrease was observed from 10 to 20 nM ActD (Figure 2A). Over this range of ActD concentrations, levels of the GAPDH transcript (used as a control) remained relatively constant. To determine if ActD reduced endogenous CTG repeat transcription, a DM1 patient-derived fibroblast line containing over 2000 CTG repeats was tested (Chaouch et al., 2009). The DM1 patient-derived cells responded to ActD over a lower concentration range compared to HeLa cells, with a dose-dependent decrease in CUG RNA levels observed from 1 to 6 nM ActD treatment over an 18 hr treatment (Figure 2B). CUG RNA levels were reduced by 44% at 3 nM and 60% at 6 nM ($p = 0.03$). Interestingly, a reproducible 20% increase in CUG RNA was observed around 7 nM treatment but was significantly lower than in untreated DM1 cells. CUG repeat RNA remained constant from 7 nM to > 100 nM ActD treatment (data not shown). Once again, GAPDH control levels were unaffected by ActD levels in this concentration range. The concentrations of ActD appeared to be mildly toxic to HeLa cells at the concentrations tested, and very little to no toxicity was observed in the DM1 patient-derived fibroblast line, as confirmed by cell viability assays (data not shown).

CUG Repeat Foci Formation Is Reduced with Actinomycin D Treatment

To directly demonstrate the effect of ActD on MBNL1 sequestration, CUG foci formation and nuclear MBNL1 localization were examined in the HeLa cell system in the presence or absence of ActD. MBNL1 antibody MB1a (4A8) was used to probe for MBNL1 localization as previously described, and a CAG probe was employed to bind CUG RNA (Holt et al., 2007). Untreated HeLa cells (without CUG repeats) demonstrated diffuse localization of MBNL1 throughout the nucleus (Figure 2C, top row). In the presence of CUG_{960}, RNA foci were observed, and MBNL1 staining demonstrated aggregation (Figure 2C, middle row). Upon incubation with 10 nM ActD for 18 hr, we observed a decrease in the number of foci per cell when compared to the transfected controls (Figure 2C, bottom row). While most cells treated with this ActD concentration still possessed some nuclear foci, there was a 50% reduction observed in the number of foci per nucleus ($n = 66$, $p = 0.00002$). Furthermore, treated cells demonstrated a 46% decrease in the number of large foci, when large foci were defined as greater than 2 μm^3 ($n = 66$, $p < 0.000025$). Nuclear MBNL1 in treated cells was more diffuse compared to untreated cells, despite the persistence of several foci. Our observations of foci reduction in the HeLa model and the reduction of CUG RNA in both cell types motivated further investigations to determine if ActD treatment could correct DM1 molecular pathology in a mouse model.

Actinomycin D Partially Rescues Mis-splicing of Multiple Events in a DM1 Mouse Model

The HSA^{LR} mouse model expresses 220 CUG repeats under the human skeletal actin promoter (Mankodi et al., 2000). qRT-PCR showed a significant reduction ($p = 0.01$) of the HSA transgene mRNA in the HSA^{LR} mouse in response to a 5-day 0.025 mg/kgActD treatment compared to PBS-treated controls (Figure 3A). In contrast, mRNA levels of the endogenous *Dmpk* gene (which does not possess long repeats in these transgenic mice) did not decrease significantly upon ActD treatment (Figure 3B), suggesting specificity for the repeat-containing HSA transgene.

Splicing rescue of two commonly examined, MBNL-regulated transcripts was observed upon ActD treatment in a DM1 transgenic mouse model: the muscle-specific chloride ion channel (*Clcn1*), the mis-splicing of this event is responsible for causing the myotonia phenotype in HSA^{LR} mice, and the sarco/endoplasmic reticulum Ca^{2+} ATPase 1 (*Atp2a1 or Serca1*) (Mankodi et al., 2002; Kimura et al., 2005). In *Clcn1*, ActD treatment with either 0.125 mg/kg or 0.25 mg/kg over a 5-day treatment regimen resulted in the robust rescue of *Clcn1* splicing, as demonstrated by an increase in the exclusion of exon 7a (Figure 3C, lanes 3 and 4). The *Atp2a1* event also showed significant mis-splicing rescue. In this event, treatment with ActD increased levels of exon 22 to 83% ± 10% at the highest dosage (Figure 3D, lanes 3 and 4). Although the mis-splicing of these events never reached full rescue, the observed rescue was significant at the highest dosages. Toxicity was not observed within the mouse model over this treatment range. Other important MBNL-regulated splicing rescue events were characterized in response to ActD treatment, including *Mbnl1* (auto-regulates its own expression at the splicing level), *Vps39* (regulator of TGF-beta signaling), *Nfix* (a transcription factor), and *Ldb3* (important in membrane protein clustering). All of these events also demonstrated partial or complete rescue of mis-splicing (Figures 3F–3H). Collectively, these results showed that ActD partially reversed an important portion of DM1 molecular pathology.

ActD Does Not Globally Modify Expression Profiles of Treated DM1 Mice

Because ActD has a well-characterized ability to bind DNA ubiquitously at higher concentrations and induce global transcription inhibition, we wanted to assess ActD's effects on transcript levels at the low dosages used in these studies. Therefore, RNA-seq analyses were performed on 0.125 mg/kg, and 0.25 mg/kg ActD-treated HSA^{LR} mouse vastus muscle RNA. Only 4.3% of genes were differentially expressed ($p < 0.1$) with 0.125 mg/kg ActD treatment, compared to the untreated controls; a similarly low proportion of genes were affected with the higher treatment (0.25 mg/kg, 5.1%.) (Figure 4A). Approximately 3% of genes decreased in expression with either dosage, possibly a direct result of ActD-mediated transcriptional inhibition. Meanwhile, about 2% of genes increased in expression with either dosage. Collectively, these data demonstrated that ActD does not broadly inhibit transcription within these treatment concentrations, and does not affect a relatively large percentage of the transcriptome. Furthermore, we observed consistency in the way genes changed across the two dosages (Table S1; Figures 4B and 4C). In total, 631 genes were upregulated by either dosage, and 401 of these genes were shared across the two concentrations (Figure 4B). When comparing the fold change of these values, we observed a correlation (Pearson $r = 0.967$) between the two ActD treatments, indicating that the degree of change did not vary significantly at the higher dosage (Figure 4C). Therefore, it is clear that the 0.25 mg/kg dosage, which is required for maximal splicing rescue, does not affect significantly more transcripts compared to the 0.125 mg/kg dosage, although we anticipate that a larger dosage difference may affect a greater proportion of genes. The functional categories of genes that are changed in both ActD treatments are found in Table S2 and indicated that the gene ontology term "extracellular matrix" had a significant p value ($p = 9.22 \times 10^{-21}$).

RNA-seq data were also used to validate our previous findings that ActD rescued mis-splicing in the HSA^{LR} mouse, as well as identify additional splicing changes that resulted from ActD treatment. Differential splicing analyses were used to compare "percent spliced in" (PSI or Ψ) values of alternatively spliced cassette exons between WT and ActD-treated mice (change in splicing denoted as $\Delta\Psi$). In total, 265 skipped exon events showed evidence of mis-regulation between WT and HSA^{LR} mice ($\Delta\Psi \geq 0.05$, Bayes factor ≥ 5; Table S3). This finding was consistent with previously published results (Wang et al., 2012). Of those events, 70 were rescued to some degree with 0.25 mg/kg ActD, 53 events were rescued with 0.125 mg/kg ActD and 40 showed rescue in both dosage groups. Importantly, of the 70 events rescued at the 0.25 mg/kg dosage, the majority demonstrated greater than 50% mis-splicing rescue upon ActD treatment (Figure 5A). Three events previously examined using qRT-PCR (*Mbnl1*, *Ldb3*, and *Atp2a1*) demonstrated a clear trend toward splicing rescue as did three previously unexplored events (*Capzb*, *Igtb1*, and *Usp47*) (Figure 5B). Interestingly, the gene ontology term "alternative splicing" was among those with a low p value for both ActD concentrations ($p = 4.00 \times 10^{-10}$) for gene expression changes (Table S2).

DISCUSSION

Our results demonstrate that ActD, a known transcription inhibitor with affinity and specificity for GC-rich DNA (Kamitori and Takusagawa, 1992), reduces CUG RNA transcript levels in both DM1 cell and mouse models (Figures 2Aand 2B), and rescues MBNL1 dependent mis-splicing events in a mouse model (Figure 3). At low nanomolar concentrations, ActD reduced CUG levels in HeLa and DM1 cells by 50%, and a similar effect was observed with a 0.25 mg/kg dosage over 5 days in a DM1 mouse model. Importantly, RNA-seq results from ActD treated DM1 mice demonstrated that ActD did not affect transcription globally; at 0.25 mg/kg less than 5% of genes were altered; however, multiple mis-spliced events were partially or fully rescued with this ActD dosage (Figure 5). Taken together, these results suggest that ActD possesses specificity for the CTG/CUG repeats at this concentration, and furthermore has the ability to reverse DM1 molecular pathology.

Currently, ActD is most commonly used as a key component in the multimodal treatment of several cancer types, including Wilms tumors in children and gestational trophoblastic neoplasias in adult women (Hill et al., 2014; Osborne et al., 2011). Standard

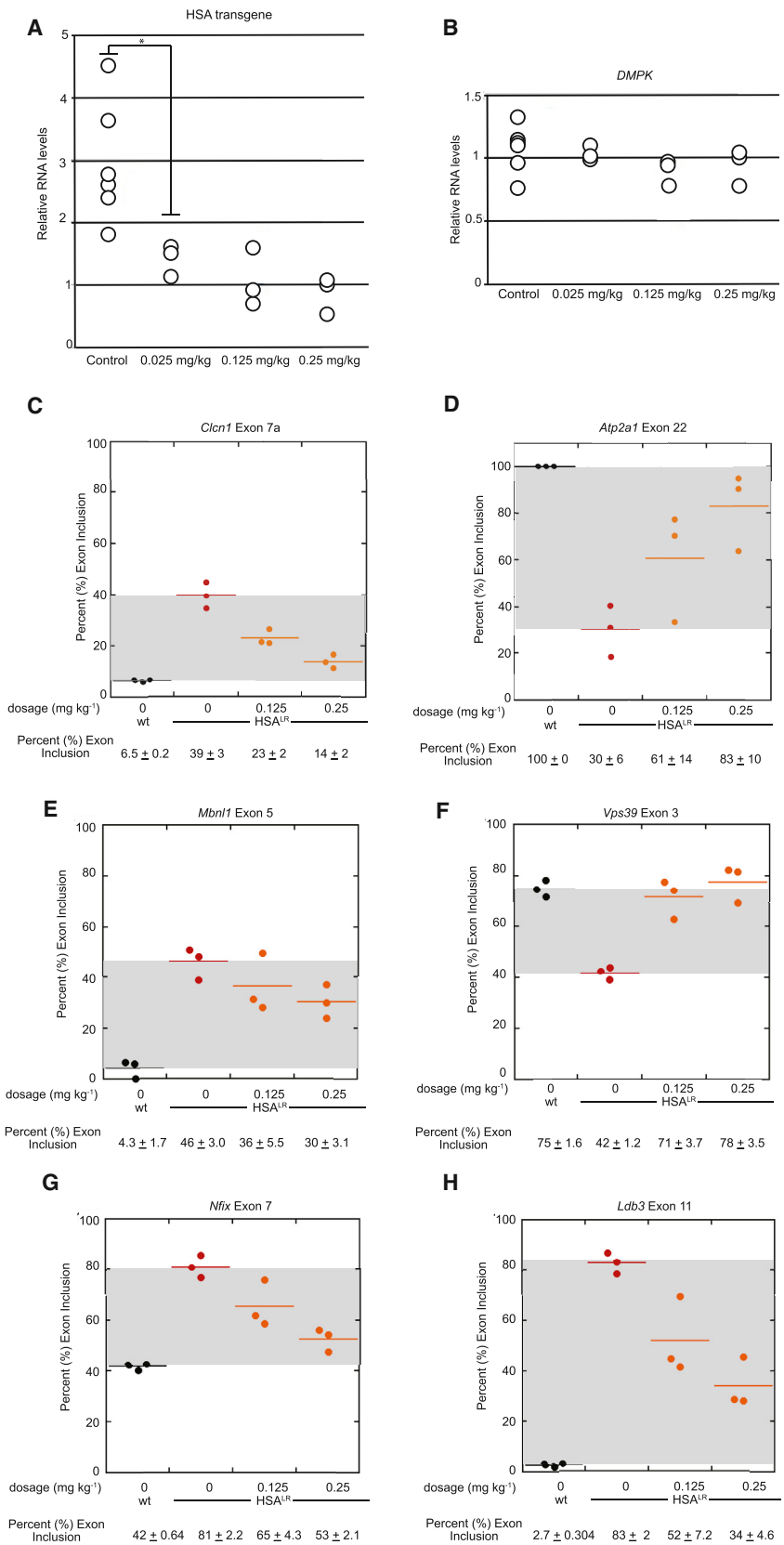

Figure 3. Actinomycin D Rescues Mis-splicing Events in HSA^{LR} Mice

(A) qRT-PCR analysis of HSA transgene levels in HSA^{LR} mice treated with PBS and 0.5% DMSO or indicated dosages of ActD for 5 days. Each circle represents the transcript levels within vastus muscle of a single mouse. Mice treated with any of the ActD dosages exhibited significant reduction of HSA transgene levels as compared to control treated mice. Asterisk indicate significance (*$p \leq 0.05$).

(B) qRT-PCR analysis of endogenous DMPK levels (no repeats) in HSA^{LR} mice treated with PBS and 0.5% DMSO or indicated dosages of ActD for 5 days. None of the ActD dosages caused significant reduction of DMPK levels.

(C–H) Jitterplot representation of various endogenous splicing events perturbed in DM1 mice. Each symbol represents the splicing outcome for vastus muscle of a single mouse, while line represents the average of all experiments.

(C) *Clcn1* splicing demonstrates almost complete rescue by 0.25 mg/kg per day for 5 days. Gel images of two replicates per condition are demonstrated below.

(D) In the *Atp2a1* event, almost full rescue is observed by 0.25 mg/kg per day for 5 days.

(E) *Mbnl1* auto-regulates exon 5 inclusion, but the highest ActD dosage only reverses ~50% of the observed mis-splicing in mice.

(F) ActD reverses mis-splicing of the *Vps39* exon 3 event completely by 0.25 mg/kg per day for 5 days.

(G and H) Nfix and Ldb3 events both exhibit partial but significant reversal of mis-splicing upon treatment with ActD.

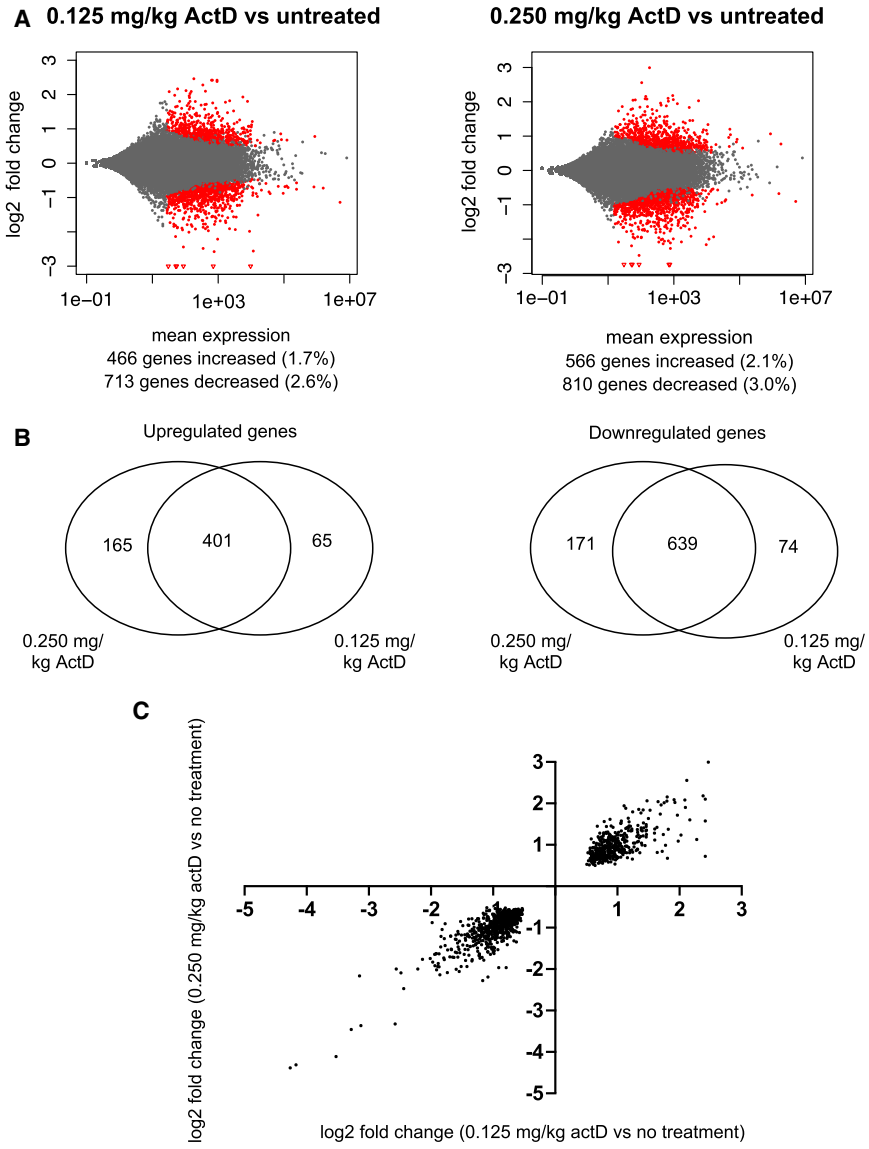

Figure 4. Less Than 5% of Genes Are Differentially Expressed in Mice upon Actinomycin D Treatment

(A) MA-plots of 0.125 mg/kg compared to no-treatment (PBS) control mice (left) and 0.250 mg/kg compared to no-treatment (PBS) control mice (right). Gene log2 fold change is plotted against the mean of normalized counts. Red circles denote genes with adjusted p values less than 0.1. Points that do not fall within the window are denoted with triangles.

(B) Venn diagram depicts the number of differentially expressed genes shared by the two treatments compared to the no-treatment control.

(C) Genes are plotted with the log2 fold change for mice treated with low (0.125 mg/kg) verses high (0.250 mg/kg) dose of ActD.

dosages of treatment for children and adults vary between 0.015 and 0.045 mg/kg. In this study, the lowest and highest dosages administered to mice were 0.025 mg/kg and 0.25 mg/kg. To extrapolate the human equivalent dosage (HED) of this treatment range, we used a body surface area normalization method, recommended as the appropriate conversion method when entering phase I and II clinical trials (Reagan-Shaw et al., 2008). This method calculates the HED of a treatment by multiplying the animal dosage by an appropriate species-specific conversion factor, or K_m, which has been previously established for a number of species used as animal models (Freireich et al., 1966). Our results demonstrated that ActD is able to reduce CUG RNA in mice with a HED value of 0.002 mg/kg and corrected mis-splicing at a HED value of 0.02 mg/kg. Both of these concentrations are below the approved therapeutic range used for Wilms tumors in standard adult patients (body weight average = 60 kg). Overall, our findings demonstrate that inhibiting transcription of CTG expansions is a promising approach for potential treatment of DM1. It will be interesting to determine if ActD can inhibit transcription of other GC-rich toxic RNAs such as CCUG repeats that cause DM2, CGG repeats that cause FXTAS and GGGGCC repeats implicated in causing ALS (Mohan et al., 2014).

We also observed a significant decrease of cellular foci in our HeLa-based DM1 model (Figure 2C). However, we interpreted these data cautiously because of the noted distinction in how ActD reduces CUG RNA in HeLa versus DM1 cellular systems. It is not clear why the reduction of CUG repeats by ActD reaches a plateau and modestly increases at higher ActD concentrations in the DM1 patient cells. Another small molecule could be added to target the remaining CUG repeats to determine if a cocktail approach could have a significant impact on CUG repeat levels. These results combined with previous work showing that diamidines reduced levels of CUG repeat RNAs in DM1 cell and mouse models (Coonrod et al., 2013; Siboni et al., 2015), suggest that targeting transcription of expanded CUG repeats and other repeat expansions should be pursued to develop lead compounds for potential therapeutics for DM and other toxic RNA diseases.

EXPERIMENTAL PROCEDURES

Isothermal Calorimetry Methods

DNA and RNA sequences were purchased from Integrated DNA Technologies. Actinomycin D was dissolved in ITC buffer Stock DNA, RNA, and ActD solutions were prepared by dissolving in ITC buffer (1× PBS, 5 mM $MgCl_2$). The oligomer samples were then heated to 90°C for 5 min followed by cooling on ice. ITC measurements were carried out on a MicroCal titration calorimeter (GE Healthcare) at 20°C. The solution in the cell (the nucleic acid) was stirred at 293 rpm by the syringe during the entire course of the experiment and the reference power of the instrument was held at 25 μCal/s. ActD was titrated

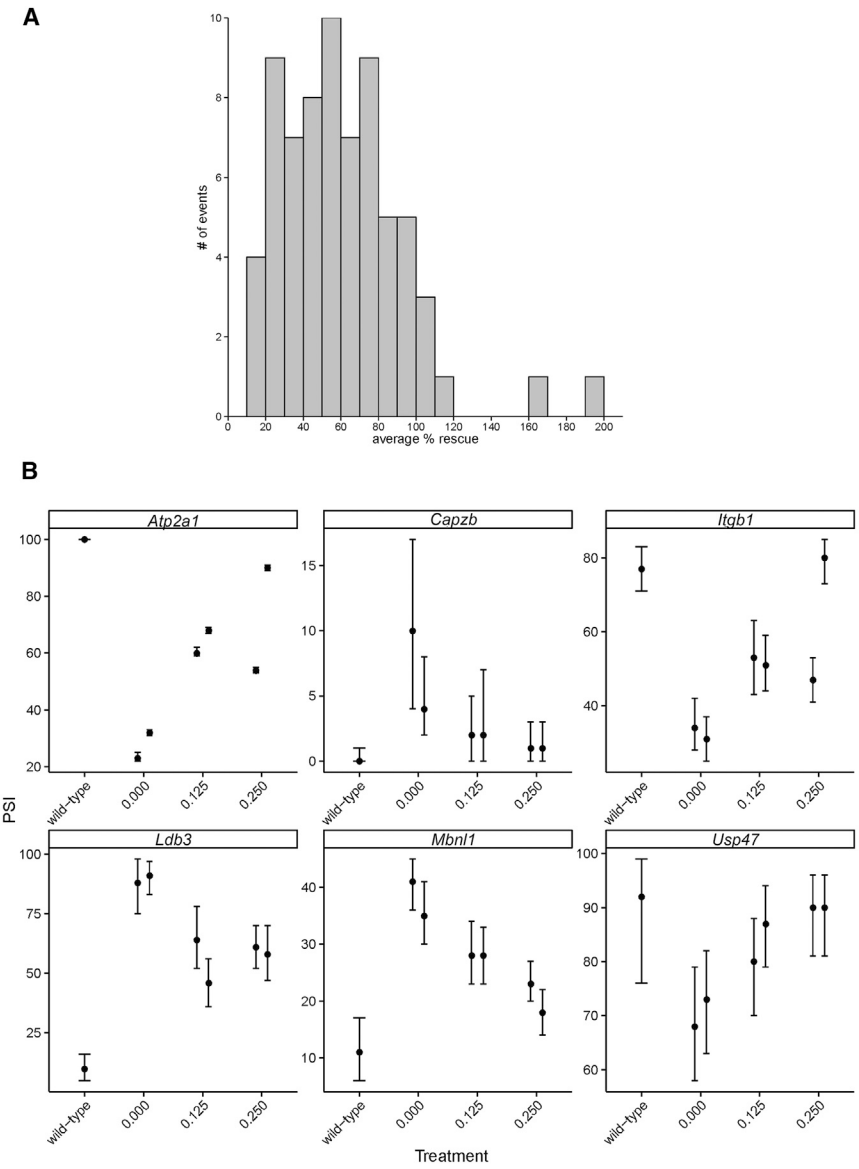

Figure 5. Numerous Mis-spliced Events Are Rescued upon Actinomycin D Treatment in DM1 Mice

(A) Distribution of the average percent rescue observed for the 70 splicing events that were mis-regulated in HSA^{LR} mice and showed evidence of rescue in littermate mice treated with 0.25 mg/kg ActD.

(B) Jitterplot representation of various splicing events perturbed in HSA^{LR} mice that showed evidence of rescue. Each symbol represents the splicing outcome estimate generated by MISO in the vastus muscle of a single mouse and the line represents the 95% confidence interval on that estimate.

in 8 μl injections with a wait time of 300 s between injections. A smaller initial injection of 4 μl was made after the initial wait time of 60 s to guarantee that only fully concentrated ActD was injected in subsequent injections. All ITC data were analyzed using Origin 7.0 software supplied by MicroCal. A non-linear least-squares fit algorithm was used with a two site, sequential binding model. One site and two independent sites models were also tested but did not fit the data as well as the sequential model.

Northern Blot Analysis

Tissue culture methods were performed as previously described (Coonrod et al., 2013). A total of 1 μg of cellular RNA was loaded onto a 1% formaldehyde denaturing agarose gel with 1× MOPS buffer (20 mM MOPS, 8 nM NaOAc, 1 mM EDTA) in northern sample buffer (67% formamide, 21% formaldehyde solution, 1× MOPS buffer). The gel was run in 1× MOPS buffer at 100 V for 4.5 hr. Gel was transferred to a 0.45 μm nylon Magna membrane (GE) and the cross-linked using a UV Stratalinker (Stratagene) on the optimal cross-link setting. Membranes were probed at 55°C overnight using radiolabeled oligos: 5′- $(CAG)_2$TCGAG$(CAG)_4$ for CUG repeats in CUG_{960} and 5′-TCCAC-CACCCTGTTGCTGTAGCCAAATTCG for GAPDH. For DM1 patient-derived cells, the following radiolabeled oligo was used: 5′- $(CAG)_7$. Blots were quantified using ImageQuant (Molecular Dynamics). The relative levels of RNA were calculated by first normalizing lanes within the same gel using the GAPDH signal, and then gels were normalized by setting the levels of repeats in the untreated cells to 1. Error was determined by calculating the SD of triplicate data.

Fluorescent Microscopy

Imaging of foci was performed as previously described (Warf et al., 2009). Briefly, HeLa cells were plated in six-well plates onto coverslips and transfected with 500 ng of CUG_{960} plasmid for each experiment. After transfection, ActD was added in the indicated concentrations and the cells were fixed with 4% PFA 16 hr later. Cells were permeabilized, then probed overnight at 37°C with a Cy3 CAG_{10} probe (IDT, IA). The next night, cells were probed overnight with the MB1a anti-MBNL1 antibody (1:5000 dilution, MDA Monoclonal Antibody Resource) in 1× PBS. Cells were washed with 1× PBS and incubated with donkey anti-mouse Alexa 488 (1:500 dilution). After being mounted onto glass slides using hard-set mounting media that contains DAPI (Vectashield), cells were imaged on an Olympus Fluoview FV1000 with a Bx61 scope. Nuclear foci for each cell were quantified using ImageJ. The number of cells scored was 35 for the CUG_{960} transfection, and 33 cells were scored when cells were treated with ActD. F test analyses were performed to determine if the datasets possessed equal or unequal variances. Appropriate t test analyses were then performed using Excel.

ActD Treatment of Mice

Mouse handling and experimental procedures were conducted in accordance with the Association for Assessment and Accreditation of Laboratory Animal Care. HSA^{LR} transgenic mice in line 20b (FVB inbred background) were previously described (Mankodi et al., 2000). Gender-matched homogeneous HSA^{LR} mice of 6–7 weeks age were treated with ActD at the indicated dose by daily intraperitoneal injection for 5 days. Control group received PBS with 0.5% DMSO. Mice were killed 1 day after the final injection and vastus lateralis muscles (quadriceps) were obtained for splicing analysis. RNA extraction, cDNA preparation, PCR amplification, and analyses on agarose gels using a fluorimager were all performed as previously described (Warf et al., 2009).

qRT-PCR

Quantitative real-time PCR was performed with TaqMan Gene Expression assays on an ABI PRISM 7900HT Sequence Detection System (Applied

Biosystems) and analyzed using the Quantitative-Comparative (C_T) method. The levels of human skeletal actin (HSA) mRNA and mouse endogenous DMPK mRNA were normalized to Gtf2b mRNA and displayed graphically as relative mRNA levels.

RNA-Seq

Whole-tissue RNA was TRIzol extracted from quadricep muscle of two age-matched mice treated with either no ActD (PBS), 0.125 mg/kg, or 0.25 mg/kg actinomycin D. For each sample, 10 μg of RNA were prepped, depleted of rRNA using a Ribo-Zero rRNA removal kit (Epicenter), and used to generate sequencing libraries using the ScriptSeq v2 kit (Epicenter). After PCR amplification, each of the six libraries was combined in equimolar amounts to a total of 20 nM and submitted for single-end, 75-base pair sequencing on the Illumina Next-Seq 500 massively parallel sequencer at the University of Oregon Genomics Core Facility. Illumina RNA-sequencing reads were aligned against the mm10 mouse reference genome with GSNAP, using a splice sites map file that was generated from Ensemble mm10 gene models (GRCm38.80) and allowing for splicing detection (Wu and Nacu, 2010) (http://research-pub.gene.com/gmap/). Between 48.5 and 98 million unique reads were acquired for each sample, of which ~84% mapped to the mouse genome. Gene read counts were generated with HT-Seq (Anders et al., 2015) using the Ensemble mm10 (GRCm38.80) gene model annotations and used as the input to DESeq2. Differential expression analysis was performed with DESeq2 (Love et al., 2014) using a FDR = 0.1 as a cutoff for statistical significance. Isoform abundances were estimated for each HSA^{LR} sample and compared to the pooled average of four wild-type samples (Wang et al., 2012) using MISO version 0.5.3 (Katz et al., 2010) and the mm10 alternative splicing event annotations provided by the developers of MISO (http://miso.readthedocs.org/en/fastmiso/). Functional annotations were obtained using DAVID bioinformatics resources (Huang et al., 2009a, 2009b).

ACCESSION NUMBERS

The accession number for the RNA-seq data reported in this paper is NCBI SRA: SRP064429.

SUPPLEMENTAL INFORMATION

Supplemental Information includes three tables and can be found with this article online at http://dx.doi.org/10.1016/j.celrep.2015.11.028.

AUTHOR CONTRIBUTIONS

R.B.S., M.N., and J.A.B. conceived the project, analyzed results, and wrote the manuscript. R.B.S characterized ActD treatment in cellular systems, established treatment ranges, and prepared the RNA-seq library. M.N. characterized ActD treatments in mouse systems and collected samples for RNA-seq analysis. S.D.W., M.K.T., and A.J.S. performed RNA-seq bioinformatics analysis. L.A.S. performed northern blots on DM1 cell lines. S.A.H. and D.M.C. performed isothermal calorimetry analyses.

ACKNOWLEDGMENTS

This work was supported by NIAMS/NIH grants AR0599833 and F32AR063565. We appreciate helpful advice and suggestions from members of the Berglund lab and Eric Wang.

Received: November 17, 2014
Revised: September 10, 2015
Accepted: November 6, 2015
Published: December 10, 2015

REFERENCES

Anders, S., Pyl, P.T., and Huber, W. (2015). HTSeq–a Python framework to work with high-throughput sequencing data. Bioinformatics *31*, 166–169.

Arambula, J.F., Ramisetty, S.R., Baranger, A.M., and Zimmerman, S.C. (2009). A simple ligand that selectively targets CUG trinucleotide repeats and inhibits MBNL protein binding. Proc. Natl. Acad. Sci. USA *106*, 16068–16073.

Bensaude, O. (2011). Inhibiting eukaryotic transcription: Which compound to choose? How to evaluate its activity? Transcription *2*, 103–108.

Chaouch, S., Mouly, V., Goyenvalle, A., Vulin, A., Mamchaoui, K., Negroni, E., Di Santo, J., Butler-Browne, G., Torrente, Y., Garcia, L., and Furling, D. (2009). Immortalized skin fibroblasts expressing conditional MyoD as a renewable and reliable source of converted human muscle cells to assess therapeutic strategies for muscular dystrophies: validation of an exon-skipping approach to restore dystrophin in Duchenne muscular dystrophy cells. Hum. Gene Ther. *20*, 784–790.

Chi, L.M., and Lam, S.L. (2005). Structural roles of CTG repeats in slippage expansion during DNA replication. Nucleic Acids Res. *33*, 1604–1617.

Cho, D.H., and Tapscott, S.J. (2007). Myotonic dystrophy: Emerging mechanisms for DM1 and DM2, *Biochimica et Biophysica Acta (BBA)* -. Mol. Basis Dis. *1772*, 195–204.

Coonrod, L.A., Nakamori, M., Wang, W., Carrell, S., Hilton, C.L., Bodner, M.J., Siboni, R.B., Docter, A.G., Haley, M.M., Thornton, C.A., and Berglund, J.A. (2013). Reducing levels of toxic RNA with small molecules. ACS Chem. Biol. *8*, 2528–2537.

Echeverria, G.V., and Cooper, T.A. (2012). RNA-binding proteins in microsatellite expansion disorders: mediators of RNA toxicity. Brain Res. *1462*, 100–111.

Fardaei, M., Rogers, M.T., Thorpe, H.M., Larkin, K., Hamshere, M.G., Harper, P.S., and Brook, J.D. (2002). Three proteins, MBNL, MBLL and MBXL, co-localize in vivo with nuclear foci of expanded-repeat transcripts in DM1 and DM2 cells. Hum. Mol. Genet. *11*, 805–814.

Freireich, E.J., Gehan, E.A., Rall, D.P., Schmidt, L.H., and Skipper, H.E. (1966). Quantitative comparison of toxicity of anticancer agents in mouse, rat, hamster, dog, monkey, and man. Cancer Chemother. Rep. *50*, 219–244.

Harley, H.G., Brook, J.D., Rundle, S.A., Crow, S., Reardon, W., Buckler, A.J., Harper, P.S., Housman, D.E., and Shaw, D.J. (1992). Expansion of an unstable DNA region and phenotypic variation in myotonic dystrophy. Nature *355*, 545–546.

Hill, C.R., Cole, M., Errington, J., Malik, G., Boddy, A.V., and Veal, G.J. (2014). Characterisation of the clinical pharmacokinetics of actinomycin D and the influence of ABCB1 pharmacogenetic variation on actinomycin D disposition in children with cancer. Clin. Pharmacokinet. *53*, 741–751.

Ho, T.H., Charlet-B, N., Poulos, M.G., Singh, G., Swanson, M.S., and Cooper, T.A. (2004). Muscleblind proteins regulate alternative splicing. EMBO J. *23*, 3103–3112.

Ho, T.H., Savkur, R.S., Poulos, M.G., Mancini, M.A., Swanson, M.S., and Cooper, T.A. (2005). Colocalization of muscleblind with RNA foci is separable from mis-regulation of alternative splicing in myotonic dystrophy. J. Cell Sci. *118*, 2923–2933.

Holt, I., Mittal, S., Furling, D., Butler-Browne, G.S., Brook, J.D., and Morris, G.E. (2007). Defective mRNA in myotonic dystrophy accumulates at the periphery of nuclear splicing speckles. Genes Cells *12*, 1035–1048.

Hou, M.H., Robinson, H., Gao, Y.G., and Wang, A.H.J. (2002). Crystal structure of actinomycin D bound to the CTG triplet repeat sequences linked to neurological diseases. Nucleic Acids Res. *30*, 4910–4917.

Huang, W., Sherman, B.T., and Lempicki, R.A. (2009a). Systematic and integrative analysis of large gene lists using DAVID bioinformatics resources. Nat. Protoc. *4*, 44–57.

Huang, W., Sherman, B.T., and Lempicki, R.A. (2009b). Bioinformatics enrichment tools: paths toward the comprehensive functional analysis of large gene lists. Nucleic Acids Res. *37*, 1–13.

Kamitori, S., and Takusagawa, F. (1992). Crystal structure of the 2:1 complex between d(GAAGCTTC) and the anticancer drug actinomycin D. J. Mol. Biol. *225*, 445–456.

Katz, Y., Wang, E.T., Airoldi, E.M., and Burge, C.B. (2010). Analysis and design of RNA sequencing experiments for identifying isoform regulation. Nat. Methods *7*, 1009–1015.

Kimura, T., Nakamori, M., Lueck, J.D., Pouliquin, P., Aoike, F., Fujimura, H., Dirksen, R.T., Takahashi, M.P., Dulhunty, A.F., and Sakoda, S. (2005). Altered mRNA splicing of the skeletal muscle ryanodine receptor and sarcoplasmic/endoplasmic reticulum Ca2+-ATPase in myotonic dystrophy type 1. Hum. Mol. Genet. *14*, 2189–2200.

Konieczny, P., Stepniak-Konieczna, E., and Sobczak, K. (2014). MBNL proteins and their target RNAs, interaction and splicing regulation. Nucleic Acids Res. *42*, 10873–10887.

Lee, J.E., Bennett, C.F., and Cooper, T.A. (2012). RNase H-mediated degradation of toxic RNA in myotonic dystrophy type 1. Proc. Natl. Acad. Sci. USA *109*, 4221–4226.

Liu, C., and Chen, F.M. (1996). Actinomycin D binds strongly and dissociates slowly at the dGpdC site with flanking T/T mismatches. Biochemistry *35*, 16346–16353.

Love, M.I., Huber, W., and Anders, S. (2014). Moderated estimation of fold change and dispersion for RNA-seq data with DESeq2. Genome Biol. *15*, 550.

Mahadevan, M., Tsilfidis, C., Sabourin, L., Shutler, G., Amemiya, C., Jansen, G., Neville, C., Narang, M., Barceló, J., O'Hoy, K., et al. (1992). Myotonic dystrophy mutation: an unstable CTG repeat in the 3′ untranslated region of the gene. Science *255*, 1253–1255.

Mankodi, A., Logigian, E., Callahan, L., McClain, C., White, R., Henderson, D., Krym, M., and Thornton, C.A. (2000). Myotonic dystrophy in transgenic mice expressing an expanded CUG repeat. Science *289*, 1769–1773.

Mankodi, A., Takahashi, M.P., Jiang, H., Beck, C.L., Bowers, W.J., Moxley, R.T., Cannon, S.C., and Thornton, C.A. (2002). Expanded CUG repeats trigger aberrant splicing of ClC-1 chloride channel pre-mRNA and hyperexcitability of skeletal muscle in myotonic dystrophy. Mol. Cell *10*, 35–44.

Miller, J.W., Urbinati, C.R., Teng-Umnuay, P., Stenberg, M.G., Byrne, B.J., Thornton, C.A., and Swanson, M.S. (2000). Recruitment of human muscleblind proteins to (CUG)(n) expansions associated with myotonic dystrophy. EMBO J. *19*, 4439–4448.

Mohan, A., Goodwin, M., and Swanson, M.S. (2014). RNA-protein interactions in unstable microsatellite diseases. Brain Res. *1584*, 3–14.

Müller, W., and Crothers, D.M. (1968). Studies of the binding of actinomycin and related compounds to DNA. J. Mol. Biol. *35*, 251–290.

Nakamori, M., Gourdon, G., and Thornton, C.A. (2011). Stabilization of expanded (CTG)·(CAG) repeats by antisense oligonucleotides. Mol. Ther. *19*, 2222–2227.

O'Rourke, J.R., and Swanson, M.S. (2009). Mechanisms of RNA-mediated disease. J. Biol. Chem. *284*, 7419–7423.

Osborne, R.J., and Thornton, C.A. (2006). RNA-dominant diseases. Hum. Mol. Genet. *15*, R162–R169.

Osborne, R.J., Filiaci, V., Schink, J.C., Mannel, R.S., Alvarez Secord, A., Kelley, J.L., Provencher, D., Scott Miller, D., Covens, A.L., and Lage, J.M. (2011). Phase III trial of weekly methotrexate or pulsed dactinomycin for low-risk gestational trophoblastic neoplasia: a gynecologic oncology group study. J. Clin. Oncol. *29*, 825–831.

Paramanathan, T., Vladescu, I., McCauley, M.J., Rouzina, I., and Williams, M.C. (2012). Force spectroscopy reveals the DNA structural dynamics that govern the slow binding of Actinomycin D. Nucleic Acids Res. *40*, 4925–4932.

Perry, R.P., and Kelley, D.E. (1970). Inhibition of RNA synthesis by actinomycin D: characteristic dose-response of different RNA species. J. Cell. Physiol. *76*, 127–139.

Petruska, J., Arnheim, N., and Goodman, M.F. (1996). Stability of intrastrand hairpin structures formed by the CAG/CTG class of DNA triplet repeats associated with neurological diseases. Nucleic Acids Res. *24*, 1992–1998.

Philips, A.V., Timchenko, L.T., and Cooper, T.A. (1998). Disruption of splicing regulated by a CUG-binding protein in myotonic dystrophy. Science *280*, 737–741.

Ranum, L.P., and Cooper, T.A. (2006). RNA-mediated neuromuscular disorders. Annu. Rev. Neurosci. *29*, 259–277.

Reagan-Shaw, S., Nihal, M., and Ahmad, N. (2008). Dose translation from animal to human studies revisited. FASEB J. *22*, 659–661.

Reuter, J.S., and Mathews, D.H. (2010). RNAstructure: software for RNA secondary structure prediction and analysis. BMC Bioinformatics *11*, 129.

Savkur, R.S., Philips, A.V., and Cooper, T.A. (2001). Aberrant regulation of insulin receptor alternative splicing is associated with insulin resistance in myotonic dystrophy. Nat. Genet. *29*, 40–47.

Siboni, R.B., Bodner, M.J., Khalifa, M.M., Docter, A.G., Choi, J.Y., Nakamori, M., Haley, M.M., and Berglund, J.A. (2015). Biological efficacy and toxicity of diamidines in myotonic dystrophy type 1 models. J. Med. Chem. *58*, 5770–5780.

Waksman, S.A., and Woodruff, H.B. (1940). Bacteriostatic and bacteriocidal substances produced by soil actinomycetes. Proc Soc Exper Biol *45*, 609–614.

Wang, E.T., Cody, N.A., Jog, S., Biancolella, M., Wang, T.T., Treacy, D.J., Luo, S., Schroth, G.P., Housman, D.E., Reddy, S., et al. (2012). Transcriptome-wide regulation of pre-mRNA splicing and mRNA localization by muscleblind proteins. Cell *150*, 710–724.

Warf, M.B., Nakamori, M., Matthys, C.M., Thornton, C.A., and Berglund, J.A. (2009). Pentamidine reverses the splicing defects associated with myotonic dystrophy. Proc. Natl. Acad. Sci. USA *106*, 18551–18556.

Wheeler, T.M., Leger, A.J., Pandey, S.K., MacLeod, A.R., Nakamori, M., Cheng, S.H., Wentworth, B.M., Bennett, C.F., and Thornton, C.A. (2012). Targeting nuclear RNA for in vivo correction of myotonic dystrophy. Nature *488*, 111–115.

Wu, T.D., and Nacu, S. (2010). Fast and SNP-tolerant detection of complex variants and splicing in short reads. Bioinformatics *26*, 873–881.